33rd Annual International Conference of the IEEE EMBS
Boston, Massachusetts USA, August 30 - September 3, 2011

Electroconvulsive Therapy Simulations using an Anatomically-Realistic Head Model

Siwei Bai, *Student Member*, *IEEE*, Colleen Loo, and Socrates Dokos, *Member*, *IEEE*

***Abstract*— Electroconvulsive therapy (ECT) is a highly effective treatment for severe depressive disorder. Efficacy and cognitive outcomes have been shown to depend on variations in treatment technique. A high resolution finite element model of a human head was generated from MRI scans and implemented with tissue heterogeneity and an excitable ionic neural model incorporated in the brain. The model was used to compare the effects of three common ECT electrode configurations, including the spatial profiles of electric field and excitation in the brain. The results showed that electrode placement has a significant effect in determining the spatial extent of activation in different brain regions, which would account for differences seen in clinical outcomes.**

I. Introduction

Electroconvulsive therapy (ECT) is an effective treatment for severe medication-resistant depression and other psychiatric disorders. It involves passing biphasic brief-pulse currents through electrodes on the head producing a generalized seizure [1]. Clinical research has demonstrated that variations in ECT treatment technique (such as electrode configurations) lead to different efficacy and side-effect outcomes [2], [3]. For instance, right unilateral (RUL) ECT has been shown to cause less short-term memory loss than bitemporal (BT) ECT, but is less clinically effective when given at the same electrical dose relative to seizure threshold [3]. Alternatively, some (but not all) studies have found bifrontal (BF) ECT causes fewer cognitive effects than BT ECT [2], [4], [5]. Nevertheless, the knowledge required to explain these underlying differences is still limited.

A number of existing studies have investigated the possible distribution of electric field (E-field) or current density within the brain during ECT, using computational head models [6]–[10]. However, none have compared the effects of various ECT electrode configurations on neural activation by incorporating excitable neural elements in the brain.

Previously, we proposed a new computational model to simulate and investigate direct brain excitation induced by ECT, by adopting a modified bidomain Hodgkin-Huxley formulation of ion currents [11]. But since the geometry of the previous head model was derived from downsampled computed tomography (CT) scans, the anatomical structure of the brain was not accurate. Therefore, the model could not account for local non-uniformities in current density caused by the complex geometry of the brain and regional differences in tissue conductivity [12], [13]. In addition, the skull was modeled as one homogeneous compartment with anisotropic conductivity, which was unable to accurately represent its three-layered structure: a low resistance spongiform layer between two high-resistive outer layers [14], [15].

In this study, a finite element (FE) model of the human head based on magnetic resonance imaging (MRI) was utilized to simulate direct brain excitation, including an excitable ionic neural model incorporated in the brain. The objective of the study was to compare the effects of three common ECT electrode placements by using this anatomically-accurate head model.

S. Bai and S. Dokos are with Graduate School of Biomedical Engineering, Faculty of Engineering, University of New South Wales (UNSW), Australia. C. Loo is with School of Psychiatry, UNSW, Department of Psychiatry, St George Hospital and the Black Dog Institute, Australia. Email: s.bai@student.unsw.edu.au; s.dokos@unsw.edu.au; colleen.loo@unsw.edu.au.

II. Methods

A. Image segmentation and finite element mesh generation

T1-weighted MRI scans of a healthy 35-year-old Asian male subject were obtained from Neuroscience Research Australia. The scans were sagittally oriented with voxel resolution of $1 \times 1 \times 1$ mm^3.

Head tissue masks were obtained with a combination of automated and manual segmentation softwares. Automated mask generation was performed using BrainSuite2 (www.loni.ucla.edu/Software/BrainSuite), and tissue compartments including skin, skull, cerebrospinal fluid (CSF), grey matter (GM) and white matter (WM) were generated from the MRI data. The information was then imported into ScanIP (Simpleware Ltd., UK) for manual processing, with a combination of different segmentation algorithms in the software: Masks representing eyes, paranasal sinuses, larynx and cervical vertebrae were separated from skin and skull, as shown in Fig. 1. The brain masks consisted of GM, WM, cerebellum (CB, with brainstem) and the cervical spinal cord (SC). The skull was divided into three compartments including compact bone tissue (with the jaw) and spongy bone tissue, as shown in Fig. 2. Later, to increase computational efficiency, the images were downsampled to a resolution of $1.5 \times 1.5 \times 1.5$ mm^3.

The +FE-Free meshing algorithm in ScanIP was chosen to generate the mesh, resulting in 1,126,135 elements.

B. Tissue properties

All compartments were considered electrically homogeneous and isotropic. Compartment conductivities, listed in Table I, were assigned mean values taken from multiple studies [16]–[19]. Since the paranasal sinuses are air-filled, their electrical conductivity was set to zero.

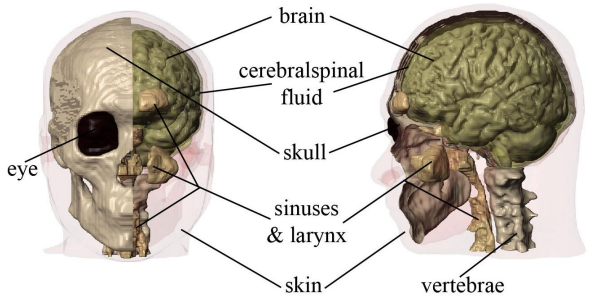

Fig. 1. Segmentation of human head: skin, eye, paranasal sinuses (with larynx), skull (including compact bone tissue and spongy bone tissue), vertebrae, CSF and brain (including GM, WM, CB and SC).

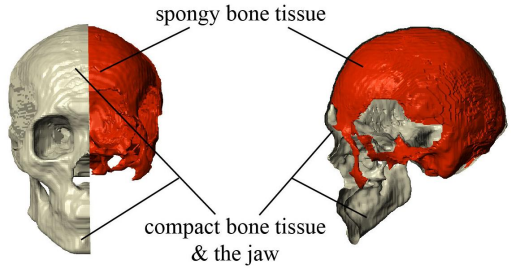

Fig. 2. Segmentation of skull: compact bone tissue and spongy bone tissue.

C. Field solver for volume conductors

ECT electrodes patched onto the scalp were defined mathematically, as detailed in Bai *et al.* [11]. Three typical electrode configurations used in clinical ECT were simulated: each utilizing two electrodes placed on the scalp, as shown in Fig. 3.

Volume compartments including GM, WM and CB were simulated by a continuum model based on the Hodgkin-Huxley formulation of ionic currents [20], implemented with Laplace's equation with non-zero volume current source. All remaining compartments were considered as passive volume conductors. Detailed descriptions of the model can be found in Bai *et al.* [11]. The electrode stimulus current waveform was a single monophasic square pulse of amplitude 800 mA and pulsewidth 1 ms, with electrode A being the anode and electrode B the cathode (Fig. 3).

TABLE I

TISSUE CONDUCTIVITIES

Compartment	Electrical Conductivity (S/m)
Scalp	0.41
Eye	0.5
Sinus (air-filled)	0
Skull (spongy bone)	0.028
Skull (compact bone)	0.006
Vertebrae	0.012
CSF	1.79
Brain (GM, CB and SC)	0.31
Brain (WM)	0.14

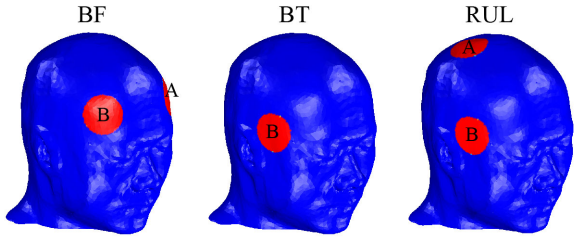

Fig. 3. Typical electrode placements used in clinical ECT application: bifrontal (BF), bitemporal (BT) and right unilateral (RUL). 'A' and 'B' are labels for the separate electrodes in each electrode placement.

The models had more than 6×10^6 degrees of freedom. They were solved in COMSOL Multiphysics (COMSOL AB, Sweden) using a segregated numerical solver on a Windows 64-bit workstation with 24 GB RAM utilizing 4 processors. To solve the time-dependent equations, a variable step backward differentiation formula (BDF) scheme was utilized with an absolute error tolerance set to 10^{-3}. It took approximately 20 hours to solve for a 6-millisecond simulation.

III. RESULTS

Fig. 4 demonstrates the E-field distributions in the brain with three different electrode configurations shown in Fig. 3. The distribution is shown with a lateral view of whole brain and two coronal slices slicing through the frontal (Fig. 4a) and temporal (Fig. 4b) lobes respectively. As expected, the regions directly beneath the electrodes had a greater E-field magnitude compared to the remainder of the brain; however, the maximum E-fields were not found on the gyri, but at the base of the sulci. Although the maxima were similar in all three configurations, the average E-fields over the entire brain volume were somewhat different: 25.4, 28.5 and 29.4 V/m for BF, BT and RUL respectively.

Fig. 5 shows the maximum extent of spatial activation of the brain, and similar to Fig. 4, it depicts a view of whole brain and two coronal slices at the same locations. Based on the profile of E-field distribution, it was to be expected that brain excitation in BF tended to cover the frontal lobe and the anterior portion of the temporal lobe, while in BT it was localized to the temporal lobe and the lateral-frontal region. Nevertheless, the location of the excited region in RUL shifted inferiorly towards the base of the right temporal lobe compared to that in BT. In addition, CB was excited in both BT and RUL, while the brainstem was activated only in RUL.

IV. DISCUSSION AND CONCLUSION

Our study simulated direct excitation of the brain induced by ECT, using an anatomically accurate head model. It compared the effects of three different electrode configurations in terms of the distribution of E-field and the spatial extent of excitation in the brain.

The strengths of the E-field were found to be of the same order of magnitude as those in prior studies [7],

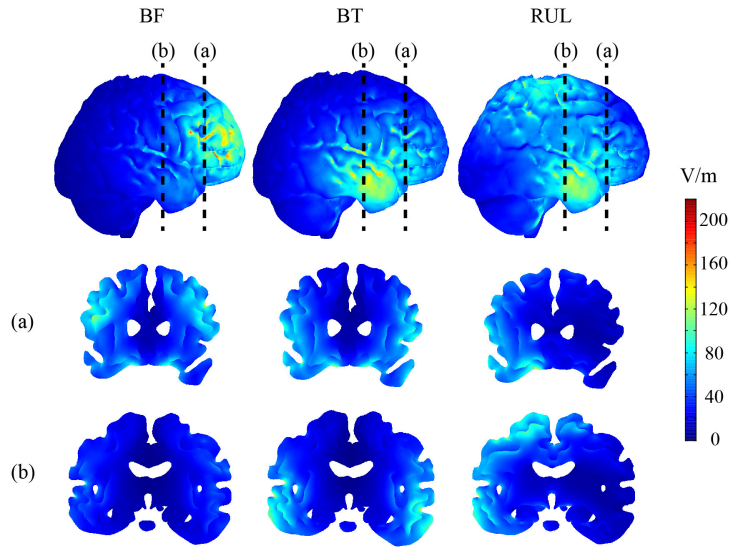

Fig. 4. Electric field magnitude (E-field) distribution in the brain with three ECT electrode configurations. The uppermost row shows the lateral view of the whole brain, and the lower two rows show the coronal slices of the brain at the same scale. Dashed lines indicate locations of slice planes.

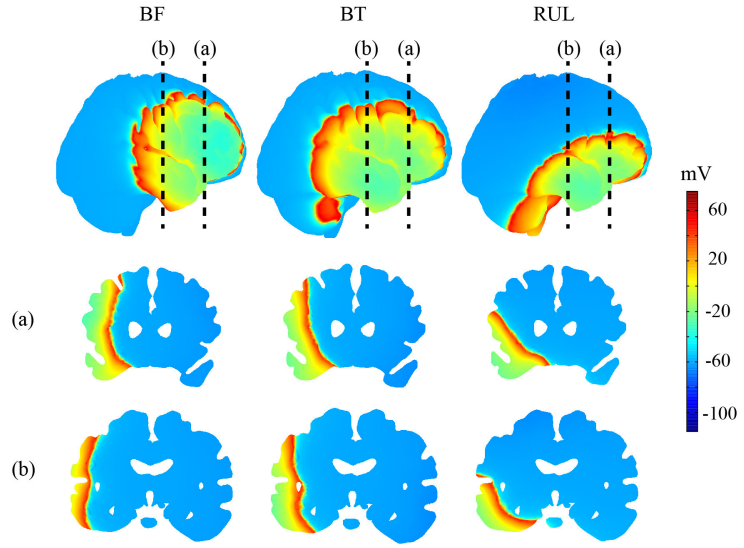

Fig. 5. Maximum brain excitation in each of the three electrode configurations, shown as the neural membrane potential throughout the brain in millivolts. The uppermost row shows the lateral view of the whole brain, and the lower two rows show the coronal slices of the brain at the same scale. Dashed lines indicate locations of slice planes.

[9]. In addition, the local non-uniform E-field profile was also supported by other studies, which was likely due to regional differences in conductance and to the presence of cortical foldings [12], [13]. As a result of the local focus of currents near the electrodes, maximum E-fields were similar among all three configurations. However, because of the closer distance between electrodes in BF, average E-field was smaller in comparison with BT and RUL.

As noted in Bai *et al*. [11], it was further demonstrated in then present study that each electrode placement plays an important role in which brain regions are maximally activated. Regions directly beneath the electrodes were found to be most excited by the applied stimulus, and the location of excitation was thus related to the spatial profile of the E-field in the brain. It should be noted that even though BT and RUL shared the same temporal electrode placement (electrode B in Fig. 3), and possessed similar E-field distributions in the temporal lobe, the location and extent of excitation differed. It is possible that such differences may influence clinical outcomes, given that with RUL less volume in the frontotemporal regions will be activated. These regions are postulated to play a critical part in mediating the effects

of antidepressant treatment [21].

Furthermore, it was unexpected that excitations were found in the CB with BT and RUL as well as in the brainstem with RUL. However, the result that the brainstem was excited in RUL concurs with recent findings indicating that RUL has greater effects on heart rate than bilateral forms of ECT [22], [23]. Also, imaging studies have found that CB was also selectively activated by ECT [24], [25], in good agreement with our results. The absence of CB excitation in our previous study [11] again demonstrated the importance of anatomical accuracy in model geometry.

Several factors may contribute to future improvements of this model. WM exhibits highly anisotropic conductivity due to axonal fibre orientation [19], [26], and therefore it is likely to enhance the complexity of spatial profiles of E-field and excitation. Another limitation is that the stimulus in this study was a monophasic pulse. However, due to the biphasic nature of the clinical ECT stimulus, an additional reverse pulse may provide more complex modes of activation. And finally, the skull produces low signals in T1-weighted MRI, and thus it is difficult to distinguish from neighboring tissues. A set of co-registered CT or photon density weighted MRI scans would be able to increase the precision in skull segmentation.

REFERENCES

[1] R. Abrams, *Electroconvulsive therapy*. Oxford University Press: New York, NY, USA, 2002.

[2] C. H. Kellner, R. Knapp, M. M. Husain, K. Rasmussen, S. Sampson, M. Cullum, S. M. McClintock, K. G. Tobias, C. Martino, M. Mueller, S. H. Bailine, M. Fink, and G. Petrides, "Bifrontal, bitemporal and right unilateral electrode placement in ECT: randomised trial," *The British Journal of Psychiatry*, vol. 196, no. 3, pp. 226–234, 2010.

[3] H. A. Sackeim, J. Prudic, D. P. Devanand, J. E. Kiersky, L. Fitzsimons, B. J. Moody, M. C. McElhiney, E. A. Coleman, and J. M. Settembrino, "Effects of stimulus intensity and electrode placement on the efficacy and cognitive effects of electroconvulsive therapy," *New England Journal of Medicine*, vol. 328, pp. 839–846, 1993.

[4] F. J. Letemendia, N. J. Delva, M. Rodenburg, J. S. Lawson, J. Inglis, J. J. Waldron, and D. W. Lywood, "Therapeutic advantage of bifrontal electrode placement in ECT." *Psychological Medicine*, vol. 23, no. 2, pp. 349–360, 1993.

[5] F. Ranjkesh, M. Barekatain, and S. Akuchakian, "Bifrontal versus right unilateral and bitemporal electroconvulsive therapy in major depressive disorder," *The Journal of ECT*, vol. 21, no. 4, pp. 207–210, 2005.

[6] Z. D. Deng, S. H. Lisanby, and A. V. Peterchev, "Effect of anatomical variability on neural stimulation strength and focality in electroconvulsive therapy (ECT) and magnetic seizure therapy (MST)." in *Proceedings of the 31st Annual International Conference of the IEEE Engineering in Medicine and Biology Society*, pp. 682–688, 2009.

[7] W. H. Lee, Z. D. Deng, T. S. Kim, A. F. Laine, S. H. Lisanby, and A. V. Peterchev, "Regional electric field induced by electroconvulsive therapy: A finite element simulation study," in *Proceedings of the 32nd Annual International Conference of the IEEE Engineering in Medicine and Biology Society*, pp. 2045–2048, 2010.

[8] Z. D. Deng, S. H. Lisanby, and A. V. Peterchev, "Electroconvulsive therapy in the presence of deep brain stimulation implants: Electric field effects," in *Proceedings of the 32nd Annual International Conference of the IEEE Engineering in Medicine and Biology Society*, pp. 2049–2052, 2010.

[9] M. Nadeem, T. Thorlin, O. P. Gandhi, and M. Persson, "Computation of electric and magnetic stimulation in human head using the 3-D impedance method," *IEEE Transactions on Biomedical Engineering*, vol. 50, no. 7, pp. 900–907, 2003.

[10] M. Sekino and S. Ueno, "FEM-based determination of optimum current distribution in transcranial magnetic stimulation as an alternative to electroconvulsive therapy," *IEEE Transactions on Magnetics*, vol. 40, no. 4 Part 2, pp. 2167–2169, 2004.

[11] S. Bai, C. Loo, and S. Dokos, "A computational model of direct brain stimulation by electroconvulsive therapy," in *Proceedings of the 32nd Annual International Conference of the IEEE Engineering in Medicine and Biology Society*, pp. 2069–2072, 2010.

[12] A. Datta, V. Bansal, J. Diaz, J. Patel, D. Reato, and M. Bikson, "Gyri-precise head model of transcranial direct current stimulation: Improved spatial focality using a ring electrode versus conventional rectangular pad," *Brain Stimulation*, vol. 2, no. 4, pp. 201–207, 2009.

[13] R. Salvador, A. Mekonnen, G. Ruffini, and P. C. Miranda, "Modeling the electric field induced in a high resolution realistic head model during transcranial current stimulation," in *Proceedings of the 32nd Annual International Conference of the IEEE Engineering in Medicine and Biology Society*, pp. 2073–2076, 2010.

[14] M. Dannhauer, B. Lanfer, C. Wolters, and T. Knösche, "Modeling of the human skull in EEG source analysis," *Human Brain Mapping*, 2011, (in press).

[15] R. J. Sadleir and A. Argibay, "Modeling skull electrical properties," *Annals of Biomedical Engineering*, vol. 35, no. 10, pp. 1699–1712, 2007.

[16] M. Akhtari, H. C. Bryant, A. N. Mamelak, E. R. Flynn, L. Heller, J. J. Shih, M. Mandelkem, A. Matlachov, D. M. Ranken, E. D. Best, M. A. DiMauro, R. R. Lee, and W. W. Sutherling, "Conductivities of three-layer live human skull," *Brain Topography*, vol. 14, no. 3, pp. 151–167, 2002.

[17] S. B. Baumann, D. R. Wozny, S. K. Kelly, and F. M. Meno, "The electrical conductivity of human cerebrospinal fluid at body temperature," *IEEE Transactions on Biomedical Engineering*, vol. 44, no. 3, pp. 220–223, 1997.

[18] C. Gabriel, S. Gabriel, and E. Corthout, "The dielectric properties of biological tissues: I. Literature survey," *Physics in Medicine and Biology*, vol. 41, p. 2231, 1996.

[19] L. A. Geddes and L. E. Baker, "The specific resistance of biological material - a compendium of data for the biomedical engineer and physiologist," *Medical and Biological Engineering and Computing*, vol. 5, no. 3, pp. 271–293, 1967.

[20] A. L. Hodgkin and A. F. Huxley, "A quantitative description of membrane current and its application to conduction and excitation in nerve," *Journal of Physiology*, vol. 117, no. 4, pp. 500–544, 1952.

[21] W. Drevets, J. Price, and M. Furey, "Brain structural and functional abnormalities in mood disorders: implications for neurocircuitry models of depression," *Brain Structure and Function*, vol. 213, no. 1, pp. 93–118, 2008.

[22] J. Nagler, "Absence of asystole during bifrontal stimulation in electroconvulsive therapy," *The Journal of ECT*, vol. 26, no. 2, p. 100, 2010.

[23] P. Stewart, C. Loo, R. MacPherson, and D. Hadzi-Pavlovic, "The effect of electrode placement and pulse width on asystole and bradycardia during electroconvulsive therapy stimulus," *International Journal of Neuropsychopharmacology*, 2011, (in press); doi: 10.1017/S1461145710001458.

[24] H. Blumenfeld, M. Westerveld, R. B. Ostroff, S. D. Vanderhill, J. Freeman, A. Necochea, P. Uranga, T. Tanhehco, A. Smith, J. P. Seibyl, R. Stokking, S. C., S. S. Spencer, and I. G. Zubal, "Selective frontal, parietal, and temporal networks in generalized seizures," *NeuroImage*, vol. 19, no. 4, pp. 1556–1566, 2003.

[25] H. Blumenfeld, K. A. McNally, R. B. Ostroff, and I. George Zubal, "Targeted prefrontal cortical activation with bifrontal ECT," *Psychiatry Research: Neuroimaging*, vol. 123, no. 3, pp. 165–170, 2003.

[26] H. Hallez, B. Vanrumste, R. Grech, J. Muscat, W. De Clercq, A. Vergult, Y. D'Asseler, K. P. Camilleri, S. G. Fabri, S. Van Huffel, and I. Lemahieu, "Review on solving the forward problem in EEG source analysis," *Journal of NeuroEngineering and Rehabilitation*, vol. 4, no. 1, p. 46, 2007.